Monolithically integrated dye-doped PDMS long-pass filters for disposable on-chip fluorescence detection

Oliver Hofmann,[a] Xuhua Wang,[ab] Alastair Cornwell,[b] Stephen Beecher,[b] Amal Raja,[c] Donal D. C. Bradley,*[b] Andrew J. deMello[c] and John C. deMello*[c]

Received 10th March 2006, Accepted 17th May 2006
First published as an Advance Article on the web 9th June 2006
DOI: 10.1039/b603678c

We report the fabrication of high quality monolithically integrated optical long-pass filters, for use in disposable diagnostic microchips. The filters were prepared by incorporating dye molecules directly into the microfluidic chip substrate, thereby providing a fully integrated solution that removes the usual need for discrete optical filters. In brief, lysochrome dyes were added to a poly(dimethylsiloxane) (PDMS) monomer prior to moulding of the microchip from a structured SU-8 master. Optimum results were obtained using 1 mm layers of PDMS doped with 1200 μg mL^{-1} Sudan II, which resulted in less than 0.01% transmittance below 500 nm (OD 4), >80% above 570 nm, and negligible autofluorescence. These spectral characteristics compare favourably with commercially available Schott-glass long-pass filters, indicating that high quality optical filters can be straightforwardly integrated into the form of PDMS microfluidic chips. The filters were found to be robust in use, showing only slight degradation after extended illumination and negligible dye leaching after prolonged exposure to aqueous solutions. The provision of low cost high quality integrated filters represents a key step towards the development of high-sensitivity disposable microfluidic devices for *point-of-care* diagnostics.

Introduction

A major goal of microfluidics research is the development of integrated systems that successfully incorporate all stages of a complete chemical or biological analysis into a single device.[1–3] Typical stages in an analysis include sampling, pre-treatment, chemical reactions, analytical separations, and analyte detection. The final step is often the most challenging due to the small quantities of analyte present and the consequent need for high sensitivity detection. In practice, optical techniques – most notably fluorescence-based detection – are often the only ones that provide adequate sensitivity,[4] and considerable efforts have therefore been devoted to developing integrated optical components for use in microfluidic devices.[5] In this regard, efforts have been made to integrate, amongst other things, prisms, microlenses, filters, mirrors, gratings, waveguides, light sources and photodetectors.[6–9]

In the context of microfluidic devices, optical long-pass filters play a particularly important role. In conventional fluorescence detection, the excitation source and detector are usually arranged orthogonally to one another to prevent direct illumination of the detector by the excitation source. This orthogonal geometry, however, is difficult to implement in a microfluidic environment since it requires the production of optical grade side-surfaces and the non-facile integration of optical components onto the side-surfaces of the microfluidic chip. The light source and detector are most conveniently located on the upper and lower faces of the microfluidic chip in a co-linear geometry, but this would ordinarily flood the detector with direct light from the excitation source, masking the typically weak fluorescence signal from the analyte. The key to achieving effective discrimination of the excitation and emission light in this 'head-on' configuration is the use of a long-pass filter in front of the detector, which blocks the excitation light and passes only the longer wavelength emission signal. The use of long-pass filters for this purpose is well established, but has generally relied on discrete stand-alone filters[10–13] – an approach which yields satisfactory optical performance but prevents monolithic integration and increases the distance between the microchannel and the detector, leading to inefficient collection of the fluorescence signal.

In this respect, it is preferable to use integrated filters that are monolithically attached to either the photodetector or the substrate of the microfluidic chip. Surprisingly, these approaches have been little used in the literature,[14,15] but fully integrated filters for silicon-based microfluidic devices have been reported by Burns *et al.*, who fabricated monolithically integrated multilayer interference filters on top of PIN silicon photodiodes.[16,17] The interference filters typically comprised up to 40 alternating layers of SiO_2/TiO_2 with ~5% transmittance at 490 nm and ~90% transmittance at 510 nm,[18] and led to significant performance gains when incorporated into DNA analysis chips. Whilst the performance of these integrated filters was somewhat impaired due to their deposition on top of a PIN diode, interference filters generally have excellent characteristics in terms of blocking, transmission, sharp roll-on, and low autofluorescence (although the angular dependence of the filter characteristics can sometimes be an issue).

[a]*Molecular Vision Ltd, 90 Fetter Lane, London, United Kingdom EC4A 1JP*
[b]*Department of Physics, Imperial College London, South Kensington, London, United Kingdom SW7 2AZ. E-mail: d.bradley@imperial.ac.uk*
[c]*Department of Chemistry, Imperial College London, South Kensington, London, United Kingdom SW7 2AZ. E-mail: j.demello@imperial.ac.uk*

However, they are expensive to produce due to their complex fabrication, and hence are ill-suited to low cost disposable applications. An alternative lower cost approach was reported by Chediak *et al.*, who developed integrated colour filters for microfluidic devices using thin-film cadmium sulfide that was deposited directly on top of PIN silicon photodiodes by pulsed laser deposition.[19] The CdS filters exhibited strong blocking of the excitation light but relatively low transmission of the emission light (~40%). In addition, although this was not specifically mentioned in ref. 19, thin film CdS is known to be highly fluorescent,[20] so it is likely that these filters would have exhibited strong autofluorescence – a serious issue for on-chip detection as discussed below.

There have been few, if any, reports of optical filters that are monolithically integrated with the substrate of the microfluidic chip. The interference-filters and CdS-filters described above could, in principle, be straightforwardly integrated with glass microfluidic chips, but they are unsuitable for conformable elastomeric materials such as PDMS – a preferred substrate material for low cost disposable applications[21,22] – since polycrystalline materials such as CdS, TiO_2 and SiO_2 are typically deposited at relatively high temperatures (>300 °C) and have a tendency to crack when the substrate is flexed. One possible approach for low cost flexible applications has been described by Whitesides and co-workers, who demonstrated the successful sub-surface staining of pre-polymerized PDMS by direct immersion in dye solutions (although in their case this was not done for the specific purpose of creating optical filters).[23,24] In practice, however, staining methods are poorly suited to filter fabrication since they typically result in shallow non-uniform dye incorporation and offer only limited control over the concentration of the incorporated dye. A preferable approach – although one that has not, to our knowledge, been reported in the literature – is to coat the substrate with an appropriate absorbing medium, as typically used for example in the preparation of colour LCD displays. This, however, potentially adds significant bulk to the final size of the microfluidic chip, since relatively large optical pathlengths are typically required to achieve adequate blocking of the short wavelength light.

All the above approaches introduce additional steps of varying complexity into the fabrication process. In this paper we take a different approach, which requires no extra processing steps and introduces no additional bulk or complexity to the device. In our method, lysochrome dyes are dissolved in a small volume of apolar solvent and added to the PDMS monomer prior to polymerization over a master comprising the microfluidic layout. The coloured substrate thereby obtained is able to serve concurrently as the microchannel medium and optical filter, negating the need for an additional filter layer, and allowing for improved collection of the fluorescence signal since the detector can be placed in closer proximity to the channel (Fig. 1).

The dispersal of dye molecules in polymer matrices to produce colour filters is well established, but the successful utilization of this approach to produce a dual-functioning microfluidic chip and colour-filter presents a number of challenges: (i) the co-linear detection geometry and typically weak analyte emission necessitate a sharp filter cut-on with excellent blocking and transmission on either side; (ii) due to the close proximity of the filter and photodetector, filter autofluorescence must be negligible since it is liable to raise the background signal from the photodiode and thus mask the analyte signal; (iii) the incorporation of dye molecules into the host matrix must conserve the processability of the polymer, enabling high quality microfluidic chips to be fabricated from the dye-doped polymer; and (iv) the resultant coloured substrates must be stable (on the timescale of the experiment) against dye leaching due to solvent flow through the channel. The aim of this work, therefore, was to fabricate high quality integrated microchip filters which retain the excellent processability of standard undoped PDMS and exhibit comparable optical characteristics to state-of-the-art commercial filters.[18] In previous studies, we have demonstrated the successful use of organic LEDs (OLEDs) and photodiodes as integrated light-sources for use in microfluidic-based detection schemes.[25–27] Such devices, when used in combination with the integrated filters described here, may offer a means of creating completely monolithic ultra low-cost microfluidic devices suitable for use in disposable diagnostic *point-of-care* devices.[28]

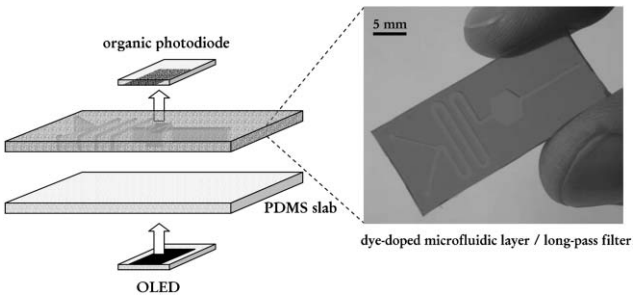

Fig. 1 Schematic of monolithically integrated optical long-pass filter use. The structured dye-doped PDMS layer serves concurrently as a microfluidic circuit and optical long-pass filter. Enclosed microchannels are obtained by sealing the doped layer against a second non-doped PDMS slab. For a co-linear detection geometry the excitation source and detector are positioned below and above the assembled microchip. The photograph shows a Sudan II doped PDMS filter with 800 μm wide and 800 μm deep microchannels.

Results and discussion

Filter fabrication

Initial experiments were focused on optimizing chromophore incorporation into the PDMS host matrix. For the purpose of comparison, following Whitesides and co-workers, post-polymerization staining with polar dyes was tested with Rhodamine B and Rhodamine 640. While for both dyes staining was apparent after immersion in aqueous dye solutions for 48 hours, a cross-sectional cut revealed heavy staining only near the surfaces, consistent with a diffusion-limited staining process. Attempts to increase the dye intake by plasma treatment of the PDMS surface prior to staining to enhance hydrophilicity and hence surface wettability, or by increasing the monomer/hardener ratio from 10 : 1 to 50 : 1 v/v to enlarge pore sizes, were unsuccessful.

It was found that improved uniformity of dye-doping could be achieved by adding the dye molecules to the

monomer/hardener mix prior to curing. For the PDMS host matrix, this required apolar chromophores since the Sylgard monomer is dissolved in hexane and xylene. Addition of polar dyes dissolved in water or ethanol resulted in emulsive non-uniform dye incorporation and incomplete polymerization. In contrast, apolar Sudan dyes dissolved well in small volumes of toluene and were uniformly incorporated after thorough mixing with the PDMS monomer and hardener. In detail, to fabricate the optical long-pass filters, Sudan II, III and IV dyes (Sigma–Aldrich, Gillingham, UK) were dissolved in ~1 mL of toluene and then added to 16.5 mL of PDMS monomer and hardener, pre-mixed at a ratio of 10 : 1 v/v (Sylgard 184 Silicone Elastomer kit, Dow Corning, Coventry, UK). Vigorous manual mixing was continued until a uniform PDMS colouring was observed. The doped PDMS was then poured into plastic Petri dishes for fabrication of unstructured filters. PDMS curing was performed at room temperature for 48 hours. Filters were prepared at various thicknesses (1–3 mm) and dye-loadings (60–1800 μg mL^{-1}). The highest dye loads necessitated an increase of the toluene content in order to achieve full dissolution of the dye molecules and uniform dispersion in the final matrix. However, excessively high solvent content resulted in incomplete polymerization even after prolonged curing. The overall solvent content in the doped PDMS was thus limited to below 10% v/v. For high dye loads, a 4 hour 65 °C curing step was added to ensure complete hardening of the PDMS.

The transmission characteristics of the dye-doped PDMS filters were measured on a UV-Vis spectrophotometer V-560 (Jasco, Great Dunmow, UK) equipped with a customized thin-film holder. Spectra were baseline corrected and referenced against air. Typical scans were performed from 250 to 850 nm at 400 nm min^{-1} with 2 nm resolution. Measurements were limited by the spectrophotometer signal-to-noise to approximately 0.001% transmittance. The transmission characteristics of the Sudan doped PDMS layers after curing are shown in Fig. 2, and are similar to those of the corresponding dye molecules in toluene. The lower transmission of the doped layers below 300 nm can be attributed to strong UV absorption by the PDMS matrix.

The ideal filter should provide excellent attenuation and transmission either side of the cut-on, and we therefore used the convenient figure of merit $Q = T(\lambda_{transmit})/T(\lambda_{block})$ to assess the filter performance, where $T(\lambda)$ is the percentage transmission at a wavelength λ, and $\lambda_{transmit}$ and λ_{block} correspond to convenient wavelengths either side of the filter cut-on.† Q corresponds to the expected improvement in sensitivity when clear PDMS is replaced by the dye-doped PDMS if the following criteria are met: (i) the spectrum of the

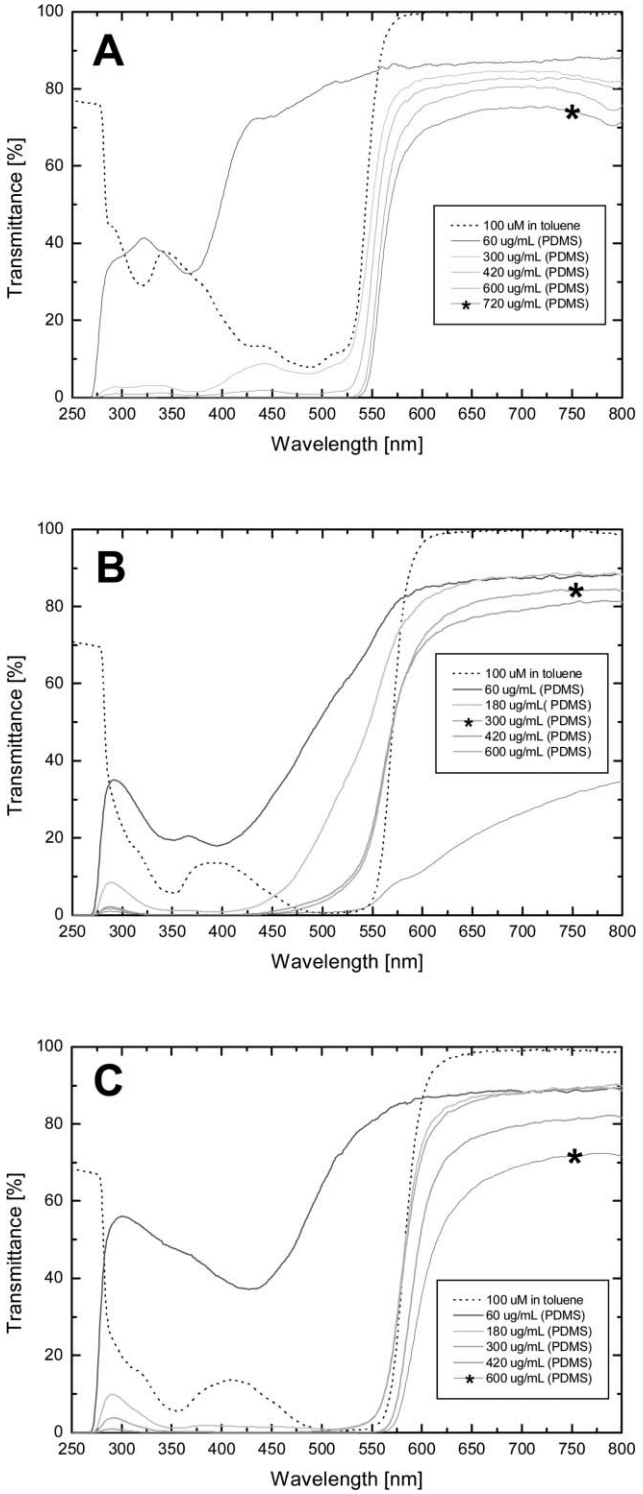

Fig. 2 Transmission characteristics of 3 mm PDMS layers doped with varying concentrations of Sudan II (A), Sudan III (B) and Sudan IV (C) dyes. The asterisks denote spectra for filters with optimized "Q-values" as defined in the main text. For comparison, the transmission characteristics of Sudan II, Sudan III and Sudan IV molecules in toluene are also shown (dotted lines). The cut-on of each dye-doped layer corresponds closely to the cut-on of the corresponding molecule in toluene. The relatively high short-wavelength transmittance of the dye molecules in toluene is due solely to the low dye molecule concentration (100 μM compared to millimolar concentrations for the doped PDMS layers) and, at high concentrations, strong short-wavelength blocking is observed in solution also.

† Note, a more rigorous figure of merit would take into account the wavelength dependence of the absorption spectrum, *i.e.*

$$Q = \frac{\left(\int_0^\infty I_{analyte}(\lambda)T(\lambda)d\lambda\right)/\left(\int_0^\infty I_{analyte}(\lambda)d\lambda\right)}{\left(\int_0^\infty I_{exc}(\lambda)T(\lambda)d\lambda\right)/\left(\int_0^\infty I_{exc}(\lambda)d\lambda\right)}$$

where $I_{exc}(\lambda)$ and $I_{analyte}(\lambda)$ represent the emission spectrum of the light source and analyte respectively. This quantity however requires advanced knowledge of the light source and analyte used in conjunction with the filter, and is therefore not suitable for generic optimisation.

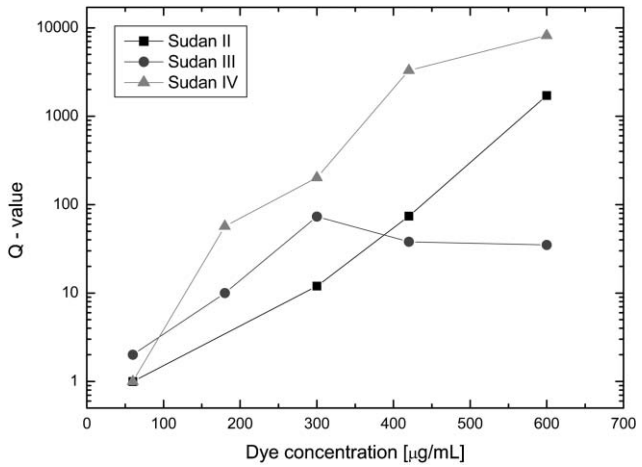

Fig. 3 The figure of merit, Q, for 3 mm PDMS layers doped with varying concentrations of Sudan II, Sudan III and Sudan IV. Q corresponds to the ratio of filter transmission at wavelengths above and below the cut-on point. For Sudan II (cut-on 550 nm) transmission values at 600 and 500 nm were used. For Sudan III (cut-on 560 nm) and Sudan IV (cut-on 580 nm), transmissions at 650 and 470 nm, and 630 and 530 nm were used, respectively.

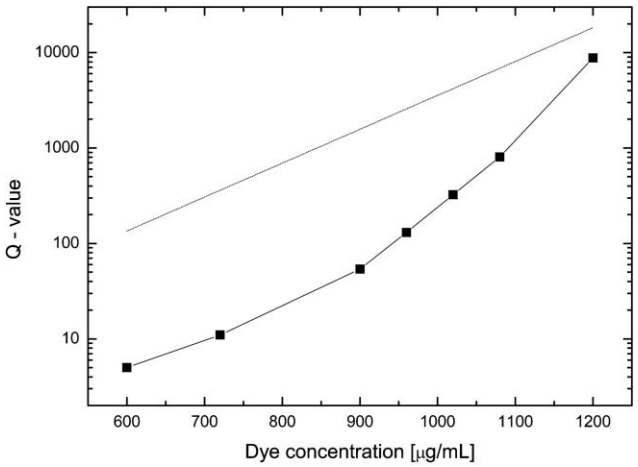

Fig. 4 The figure of merit, Q, for 1 mm PDMS layers doped with varying concentrations of Sudan II. The dotted line corresponds to the theoretical limit based on the extinction coefficient of Sudan II above and below the cut-on point.

light source lies entirely in the attenuation region of the long-pass filter; (ii) the analyte emission spectrum lies entirely in the transmissive region of the long-pass filter; (iii) the limit-of-detection is determined by the background due to the excitation light rather than detector noise or other electronic noise; and (iv) the autofluorescence from the filter is negligible. If these criteria are satisfied then the optimal filter performance is obtained at the dye loading that maximises Q.

In preliminary tests, to assess the relative performance of the three dye molecules, 3 mm thick filters were fabricated using Sudan II, Sudan III and Sudan IV dye loadings in the range 60 to 720 μg mL^{-1}. The concentration dependence of the Q values for the three dyes are shown in Fig. 3. The Q values for Sudan II and Sudan IV increase rapidly with dye-loading, consistent with improved short wavelength attenuation as the dye concentration increases. In the case of Sudan III, the Q value at first increases exponentially with dye loading but rapidly reaches a peak at 300 μg mL^{-1}, and then decreases. This reduction in filter performance is attributable to aggregation of the dye molecules, since dye molecule particulates become visible in the doped PDMS layers at dye-loadings above 300 μg mL^{-1}, signifying non-uniform dye incorporation. Sudan II and IV are both promising filter materials but Sudan III is insufficiently soluble in toluene to achieve adequate filter performance. It is probable that an alternative solvent choice would permit high quality Sudan III filters to be fabricated, but this was not pursued further here.

A sharp roll-on between attenuation and transmission is crucial in fluorescence detection, so Sudan II filters, which have a typical roll-on transition width <50 nm, were selected for further optimization. In order to ensure efficient collection of fluorophore emission in a microfluidic environment, the distance between the fluorophore and detector should be kept small, and subsequent tests were therefore conducted on 1 mm filters, which is typical of the substrate thicknesses employed in microfluidic devices. In Fig. 4, we show the Q values obtained using Sudan II filters with dye concentrations in the range 600 to 1200 μg mL^{-1}, where the upper limit corresponds to the maximum dye loading that could be achieved without noticeable dye aggregation. The Q value increases sharply with concentration over the full concentration range, reaching a maximum value of $\sim$8800 at 1200 μg mL^{-1}. If the four criteria discussed above are satisfied, this represents a potential increase in sensitivity of almost four orders of magnitude. The Q value increases super-exponentially over the concentration range investigated, which is somewhat surprising since, if the dye were incorporated uniformly, Q would be related to the dye concentration by the following exponential relationship

$$Q = \frac{T_{\text{long}}}{T_{\text{short}}} \propto \frac{e^{-cd\varepsilon_{\text{long}}}}{e^{-cd\varepsilon_{\text{short}}}} \propto e^{cd\left(\varepsilon_{\text{short}} - \varepsilon_{\text{long}}\right)}$$

where c is the dye concentration, d is the filter thickness, and $\varepsilon_{\text{long}}$ and $\varepsilon_{\text{short}}$ represent the extinction coefficients of the dye molecule at the long and short wavelengths respectively. The extinction coefficients of Sudan II were measured in a 100 μM solution in toluene, yielding values of 24280 and 170 $M^{-1}cm^{-1}$ at 500 and 600 nm respectively. This corresponds to a maximum theoretical Q value of 18260 for 1200 μg mL^{-1} ($\sim$4 mM) Sudan II in a 1 mm layer, substantially higher than the value actually obtained in our PDMS filters. The ideal Q value as a function of dye concentration is shown as a dotted line in Fig. 4 and, as expected, the observed data lies below the calculated optimum over the entire range. The lower non-exponential nature of the experimental data suggest that the dye is incorporated non-uniformly within the host matrix, resulting in sub-optimal blocking characteristics. Microscopic studies of the polymer blend phase structure at different dye loadings are currently under way, with a view to obtaining improved dispersion of the dye, and hence Q values closer to the theoretical maximum. We note, however, that at high dye loadings the deviation between expected and measured Q is a factor of 2 only. As an alternative explanation for the observed behaviour, there may be a chemical interaction between the PDMS and

the dye molecules, leading to a concentration-dependent extinction coefficient.

Autofluorescence measurements

The use of a standard UV-Vis spectrophotometer to investigate the transmission characteristics of the filters provides valuable but incomplete information about the suitability of the filters for microfluidic applications. In contrast to the configuration employed when using a standard absorption spectrophotometer, in an integrated microfluidic device the detector is in fact placed in direct contact with the long-pass filter. If the long-pass filter exhibits appreciable autofluorescence, this is likely to be collected by the detector, masking any weak emission from the analyte. It is therefore also important to assess the fluorescence characteristics of the filters. To do so, the filters were illuminated from the front with the focused output of a tungsten halogen lamp (A2B-W-020R, Spectral Products) equipped with a monochromator (CM110, Spectral Products) and the transmitted light and autofluorescence were detected from behind using a fibre-optic coupled CCD spectrometer (S2000 with 600 μm diameter fibre, Ocean Optics). The light source, filter, and fibre were arranged in a co-linear configuration with the collection lens of the fibre-optic being placed immediately behind the filter in order to ensure optimal collection of the isotropically emitted autofluorescence. A wavelength of 500 nm was chosen to simulate the excitation light, coinciding with the absorbance band of Rhodamine B, a commonly used diagnostic fluorophore. Monochromatic light at 600 nm was used to represent the Rhodamine B emission. The recorded signals were compared to results obtained with non-doped PDMS. Fig. 5 shows the results for a 1 mm ~OD 4 Sudan II filter. As expected from Fig. 2a, the 500 nm light is strongly attenuated by the dye-doped PDMS while the 600 nm light is transmitted at a comparable level to that for the undoped PDMS (see lower plot). The upper plot shows the 500 nm data for the dye-doped PDMS on a greatly magnified scale. There is no detectable signal at 500 nm, which indicates that the 500 nm light has been successfully attenuated below the noise floor of the spectrometer. Importantly, there is no detectable light at longer wavelengths either (where any emission from the filter would occur), indicating that the filter autofluorescence is extremely weak.

A more rigorous measurement of filter autofluorescence may be obtained using an integrating sphere – a hollow sphere that has its inner surface coated with a diffusely reflecting material. When a light-source – in this case an autofluorescent filter – is placed inside an ideal integrating sphere the light is redistributed isotropically over the sphere's interior-surface, irrespective of the angular distribution of the emission. Hence, if N_Ω photons of a given wavelength are detected over a solid angle Ω, the total number, N, of emitted photons is given by $N = k_\lambda N_\Omega(4\pi/\Omega)$, where k_λ is a wavelength dependent coefficient that accounts for reflection losses in the sphere.[29] The use of an integrating sphere therefore enables the total number of photons emitted by autofluorescence to be determined from a measurement at a single location on the sphere wall, obviating the need to map out the full angular

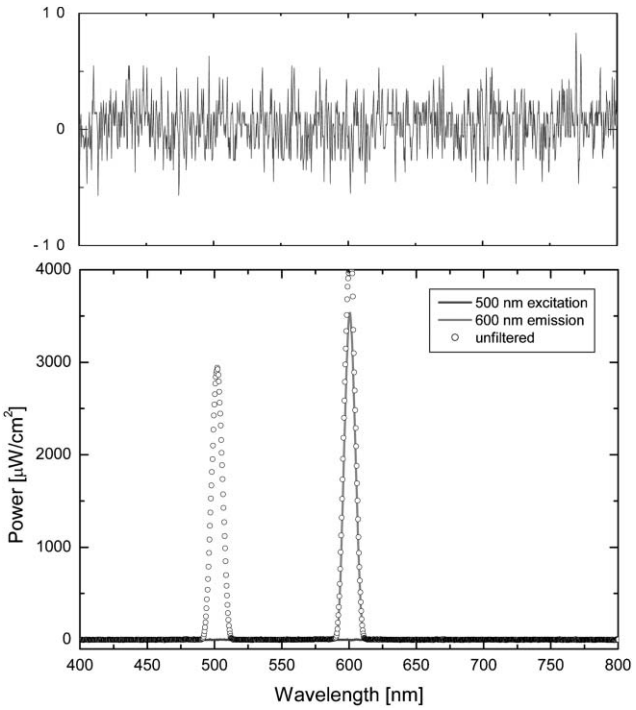

Fig. 5 The blocking properties of a 1 mm ~OD 4 Sudan II filter, measured using the co-linear configuration described in the text. The lower plot indicates that the 500 nm light is strongly attenuated by the dye-doped PDMS while the 600 nm light is transmitted at a comparable level to that for the undoped PDMS. The upper plot shows the 500 nm data for the dye-doped PDMS on a greatly magnified scale. There is no detectable signal over the full spectral range, indicating that the intensity of the transmitted light and the intensity of filter autofluorescence are both below the noise floor of the spectrometer (± 5 μW cm^{-2}).

distribution of the emission. The PDMS filters were placed inside an 18 cm diameter sphere (Labsphere) and illuminated with the 5 mW 2 mm diameter beam output from a 488 nm Ar Ion laser (43 Series Ar Ion laser, Melles Griot) entering through a small inlet port. The emitted light was detected using a fibre-optic coupled CCD spectrometer (USB 2000 CCD spectrometer with 600 μm diameter fibre, Ocean Optics) inserted into a second port, oriented at 90 degrees relative to the laser beam. The autofluorescence characteristics of the Sudan II PDMS filters were measured as well as those of a commercially available Schott-glass long-pass filter with a cut-on point at 583 nm. The Schott filter showed a small amount of autofluorescence in the range 570 to 950 nm, but no fluorescence was measurable from the PDMS filter, confirming the high quality of the Sudan II/PDMS filters (Fig. 6). Since the autofluorescence was too weak to register on the CCD spectrometer, the external photoluminescence quantum efficiency of the filter could not be calculated. However, based on the sensitivity of the system, it was certainly less than 0.01%.

Filter stability testing

To evaluate suitability of the PDMS filters for diagnostic applications, their stability against treatment with chemical solvents and prolonged light exposure was subsequently

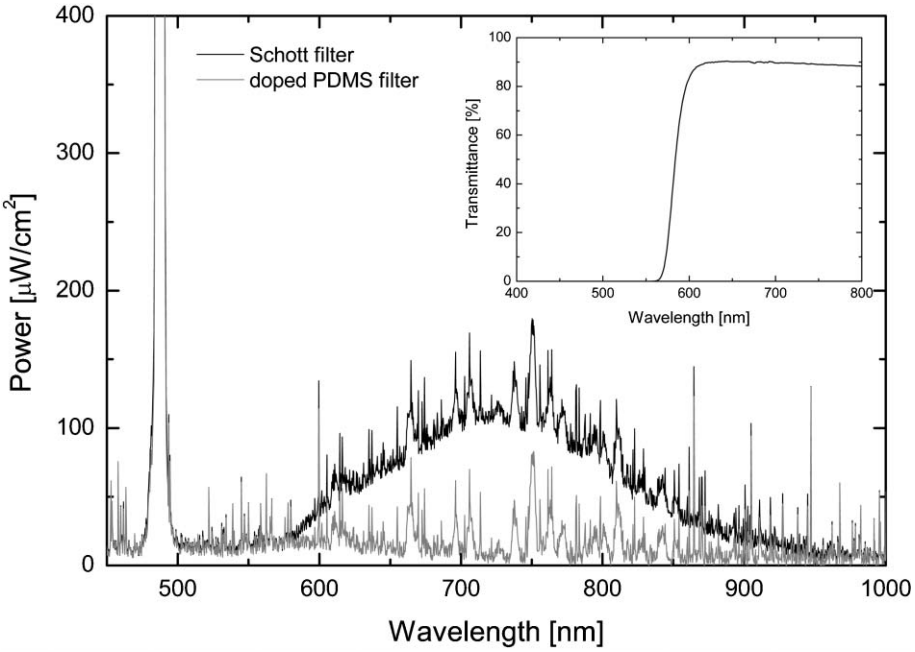

Fig. 6 Autofluorescence detection results for a 2 mm PDMS layer doped with 900 μg mL^{-1} Sudan II and a 2 mm commercial Schott-glass filter (see inset for Schott filter transmission characteristics). The dye-loading of the PDMS filter was selected to approximately match the optical density of the Schott filter for the same filter thickness. The 5 mW output from a 488 nm Ar Ion laser was used as the excitation source. Fluorescence emission was measured inside an integrating sphere with a high-sensitivity CCD spectrometer. Note: the sharp peak at 488 nm corresponds to laser light reflected from the front surface of the filter, which is also detected by the spectrometer due to the isotropic collection characteristics of the integrating sphere.

investigated (Fig. 7). For solvent stability tests, the filters were soaked in water or ethanol for up to 5 hours, or ultrasonicated in the same solvents at 33 kHz/300 W (Sonomatic S1000, Langford Electronics, Birmingham, UK). The resulting optical properties were then compared to those of untreated filters. It can be seen that ultrasonication in water for 5 min resulted in only negligible changes, with low-wavelength transmission

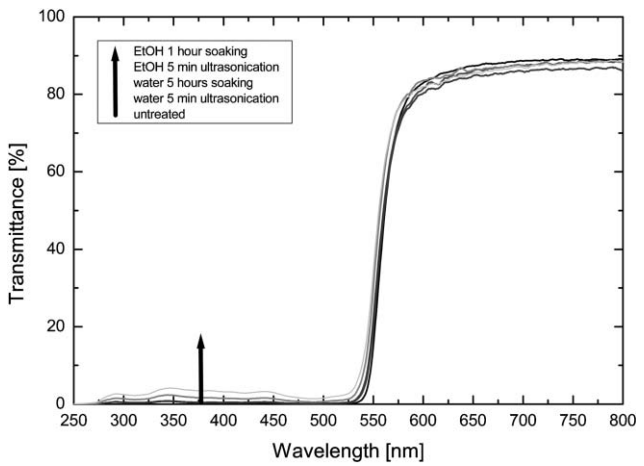

Fig. 7 Filter stability against solvent exposure. Filters were soaked or ultrasonicated in water or ethanol for different durations. Presented data is for a 2 mm PDMS layer doped with 600 μg mL^{-1} Sudan II. The short-wavelength blocking worsens as the treatment protocol changes from (i) no treatment to (ii) 5 mins ultrasonication in water to (iii) 5 hours soaking in water to (iv) 5 mins ultrasonication in ethanol to (v) 1 hour soaking in ethanol.

increased by 0.15% and high-wavelength transmission reduced by <2%. Ultrasonicating the filters in ethanol for 5 min, commonly used in microchip cleaning protocols, resulted in similar negligible transmission changes <0.6%. Soaking of the doped filters in ethanol for 1 hour resulted in a low- and high-wavelength transmission change of ~1.5%, while soaking in water for 5 hours resulted in a ~2% drop of high wavelength transmission, with negligible changes to the low wavelength blocking. We attribute these slight changes to limited dye leaching which is stronger for ethanol compared to water (due to higher Sudan dye solubility), and is enhanced by ultrasonication induced cavitation. The stability of the doped PDMS layers is clearly sufficient for disposable diagnostic applications, in which a typical measurement is expected to take no more than a few minutes.

The stability of the filters against continuous light illumination was tested by exposing the filters to ambient light in the laboratory for up to 4 weeks. Stability against UV light illumination (200 W mercury arc lamp) and blue laser light (200 mW Ar Ion laser) was also investigated. Prolonged exposure of the doped filters to ambient light in the laboratory revealed a slight deterioration of low wavelength blocking after 4 weeks, which we attribute to weak dye bleaching or aggregation (500 nm transmittance increased from <0.1 to 0.5%). Similarly, exposure to a 200W UV lamp for up to 1 hour and to a 200 mW Ar Ion laser for up to 30 min caused only minimal changes. We consider this level of photostability to be satisfactory, particularly for the anticipated use in disposable diagnostic systems which are routinely packaged in air tight aluminium foil wrapping.

Microfluidic chip fabrication

For the fabrication of monolithically integrated microfluidic/filter layers, the Sudan II doped PDMS monomer/hardener solution was poured over an SU-8 master prior to curing. The SU-8 master was fabricated on a silicon substrate using standard SU-8 processing protocols (Centre for Integrated Photonics, Ipswich, UK). The cured PDMS layer, shown in Fig. 1, was then peeled off and sealed against an unstructured slab of PDMS to form enclosed microchannels. We found that the fidelity of feature replication was unaffected by the dye doping, allowing for facile fabrication of micron-sized features. Bulk PDMS properties such as elasticity, wettability and bonding characteristics were also seemingly unaffected. The favourable properties of the PDMS were therefore retained even after dye-doping.

Conclusions

We have fabricated high quality monolithically integrated disposable PDMS based microfluidic layers with optical long-pass filter characteristics. Three lysochrome dyes were tested – Sudan II, Sudan III and Sudan IV. The Sudan III dyes had relatively low solubility in toluene and yielded poor quality filters with visibly non-uniform dye dispersion. The Sudan II and Sudan IV dyes, however, showed good solubility and yielded high quality filters with cut-on wavelengths of 550 and 580 nm, respectively. For instance, 3 mm thick filters with relatively low dye-loadings of 600 μg mL^{-1} yielded short wavelength optical densities of 3.3 and 4.3 for Sudan II and Sudan IV, respectively. The incorporation of higher dye loadings is challenging since it requires detailed optimisation of the solvent composition and curing conditions in order to achieve effective dye dispersion. However, using Sudan II as a test dye, we were able to fabricate high quality 1 mm PDMS layers with dye-loadings up to 1200 μg mL^{-1}. The resultant filters had excellent optical characteristics, *e.g.* <0.01% transmission at 500 nm and >80% transmission above 570 nm. Importantly, the filters showed negligible autofluorescence, allowing them to be effectively employed in microchip-based fluorescence detection. The filters proved robust in use, undergoing only negligible leaching in aqueous solution and marginal photodegradation. Patterning of the PDMS was unaffected by the dye doping, allowing for the fabrication of coloured substrates that serve concurrently as channel medium and optical filter. Work is ongoing to extend the range of available long-pass filters into the blue and green spectrum to match the most commonly used light sources and diagnostic fluorophores. In our efforts to develop disposable fluorescence detection systems for *point-of-care* diagnostic devices, we are also working on the fabrication of monolithically integrated short-pass filters to sharpen the output of integrated OLED light-sources.

Acknowledgements

The Imperial College authors thank the UK Engineering and Physical Sciences Research Council (GR/R58949) and Molecular Vision Ltd for funding this work. Molecular Vision Ltd acknowledges support from the UK Biotechnology and Biological Sciences Research Council through its Small Business Research Initiative (grant 147/SBRI 19689). We also thank Lesley Rivers and Rob McDougall from the Centre for Integrated Photonics, Ipswich, UK, for fabricating the SU-8 master used to mould the filters. The latter work was performed under the UK Engineering and Physical Sciences Research Council funded PRINCE project (GR/S86631).

References

1 D. R. Reyes, D. Iossifidis, P. A. Auroux and A. Manz, *Anal. Chem.*, 2002, **74**, 2623–2636.
2 P. A. Auroux, D. Iossifidis, D. R. Reyes and A. Manz, *Anal. Chem.*, 2002, **74**, 2637–2652.
3 T. Vilkner, D. Janasek and A. Manz, *Anal. Chem.*, 2004, **76**, 3373–3385.
4 A. J. de Mello, *Lab Chip*, 2003, **3**, 29N–34N.
5 K. B. Mogensen, H. Klank and J. P. Kutter, *Electrophoresis*, 2004, **25**, 3498–3512.
6 A. Llobera, R. Wilke and S. Buttgenbach, *Lab Chip*, 2004, **4**, 24–27.
7 J. Hubner, K. B. Mogensen, A. M. Jorgensen, P. Friis, P. Telleman and J. P. Kutter, *Rev. Sci. Instrum.*, 2001, **72**, 229–233.
8 J. C. Roulet, R. Volkel, H. P. Herzig, E. Verpoorte, N. F. de Rooij and R. Dandliker, *Anal. Chem.*, 2002, **74**, 3400–3407.
9 E. Verpoorte, *Lab Chip*, 2003, **3**, 42N–52N.
10 M. L. Chabinyc, D. T. Chiu, J. C. McDonald, A. D. Stroock, J. F. Christian, A. M. Karger and G. M. Whitesides, *Anal. Chem.*, 2001, **73**, 4491–4498.
11 T. Kamei, B. M. Paegel, J. R. Scherer, A. M. Skelley, R. A. Street and R. A. Mathies, *Anal. Chem.*, 2003, **75**, 5300–5305.
12 H. F. Li, J. M. Lin, R. G. Su, K. Uchiyama and T. Hobo, *Electrophoresis*, 2004, **25**, 1907–1915.
13 R. F. Renzi, J. Stamps, B. A. Horn, S. Ferko, V. A. VanderNoot, J. A. A. West, R. Crocker, B. Wiedenman, D. Yee and J. A. Fruetel, *Anal. Chem.*, 2005, **77**, 435–441.
14 E. Thrush, O. Levi, W. Ha, K. Wang, S. J. Smith and J. S. Harris, *J. Chromatogr., A*, 2003, **1013**, 103–110.
15 M. L. Adams, M. Enzelberger, S. Quake and A. Scherer, *Sens. Actuators, A*, 2003, **104**, 25–31.
16 M. A. Burns, B. N. Johnson, S. N. Brahmasandra, K. Handique, J. R. Webster, M. Krishnan, T. S. Sammarco, P. M. Man, D. Jones, D. Heldsinger, C. H. Mastrangelo and D. T. Burke, *Science*, 1998, **282**, 484–487.
17 J. R. Webster, M. A. Burns, D. T. Burke and C. H. Mastrangelo, *Anal. Chem.*, 2001, **73**, 1622–1626.
18 V. Namasivayam, R. S. Lin, B. Johnson, S. Brahmasandra, Z. Razzacki, D. T. Burke and M. A. Burns, *J. Micromech. Microeng.*, 2004, **14**, 81–90.
19 J. A. Chediak, Z. S. Luo, J. G. Seo, N. Cheung, L. P. Lee and T. D. Sands, *Sens. Actuators, A*, 2004, **111**, 1–7.
20 B. Ullrich, R. Schroeder and H. Sakai, *Semicond. Sci. Tech.*, 2001, **16**, L89–L92.
21 S. K. Sia and G. M. Whitesides, *Electrophoresis*, 2003, **24**, 3563–3576.
22 A. J. Tudos, G. A. J. Besselink and R. B. M. Schasfoort, *Lab Chip*, 2001, **1**, 83–95.
23 J. A. Rogers, R. J. Jackman, O. J. A. Schueller and G. M. Whitesides, *Appl. Opt.*, 1996, **35**, 6641–6647.
24 N. Bowden, I. S. Choi, B. A. Grzybowski and G. M. Whitesides, *J. Am. Chem. Soc.*, 1999, **121**, 5373–5391.
25 J. B. Edel, N. P. Beard, O. Hofmann, J. C. DeMello, D. D. C. Bradley and A. J. deMello, *Lab Chip*, 2004, **4**, 136–140.
26 O. Hofmann, X. H. Wang, J. C. deMello, D. D. C. Bradley and A. J. deMello, *Lab Chip*, 2005, **5**, 863–868.
27 O. Hofmann, P. Miller, P. Sullivan, T. S. Jones, J. C. deMello, D. D. C. Bradley and A. J. deMello, *Sens. Actuators, B*, 2005, **106**, 878–884.
28 O. Hofmann, A. J. deMello, D. D. C. Bradley, P. Miller and X. Wang, *GIT Lab. J.*, 2004, **5**, 28–29.
29 J. C. deMello, H. F. Wittmann and R. H. Friend, *Adv. Mater.*, 1997, **9**, 230.